HHS Public Access

Author manuscript

Nat Methods. Author manuscript; available in PMC 2012 July 01.

Published in final edited form as:

Nat Methods. ; 9(1): 84–89. doi:10.1038/nmeth.1769.

Global profiling of dynamic protein palmitoylation

Brent R. Martin[1,2,3], **Chu Wang**[1], **Alexander Adibekian**[1], **Sarah E. Tully**[1], and **Benjamin F. Cravatt**[1,3]

[1]The Department of Chemical Physiology and The Skaggs Institute for Chemical Biology, The Scripps Research Institute, 10550 N. Torrey Pines Rd., La Jolla, CA 92037

Abstract

The reversible thioester linkage of palmitic acid on cysteines is known as protein S-palmitoylation, which facilitates the membrane association and proper subcellular localization of proteins. Here we report the metabolic incorporation of the palmitic acid analogue 17-octadecynoic acid (17-ODYA) in combination with stable-isotope labeling of cells (SILAC) and pulse-chase methods to generate a global quantitative map of dynamic protein palmitoylation events in cells. We distinguished stably palmitoylated proteins from those that show rapid turnover. Treatment with a serine lipase-selective inhibitor identified a special pool of dynamically palmitoylated proteins regulated by palmitoyl-protein thioesterases. This subset was enriched in oncogenes and other proteins linked to aberrant cell growth, migration, and cancer. Our method provides a straightforward way to characterize global palmitoylation dynamics in cells and confirms enzyme-mediated depalmitoylation as a critical regulatory mechanism for a specific subset of rapidly cycling palmitoylated proteins.

Protein S-palmitoylation on cysteine residues was discovered more than 30 years ago by metabolic radiolabeling of virus particles and virus-infected cells with ^{3}H-palmitate[1]. It later became evident that palmitoylation is a universal post-translational modification important for the regulation of trafficking, membrane localization, and activity of many cellular proteins[2–3]. Additionally, given the labile properties of the thioester linkage, palmitoylation is potentially reversible and susceptible to enzymatic regulation. Traditional methods for detecting palmitoylation events by metabolic radiolabeling with ^{3}H-palmitate require film exposures lasting weeks to months, which has historically impeded the study of this important post-translational modification.

Two methods were recently described for large-scale identification of palmitoylated proteins by mass spectrometry (MS)-based proteomics. The first approach, termed acyl-biotin exchange (ABE)[4], is a multi-step protocol that uses hydroxylamine to selectively cleave

[3]Corresponding authors: brentrm@umich.edu, cravatt@scripps.edu.

[2]Present Address: Department of Chemistry, University of Michigan, 930 N. University Ave., Ann Arbor, MI 48109

Author Contributions

B.R.M. and B.F.C designed research. B.R.M performed research. A.A., B.R.M., S.E.T. and C.W. contributed new analytical tools. B.R.M. and B.F.C. analyzed data and wrote the manuscript.

Supplementary Note. Synthetic methods

thioester bonds on proteins, followed by disulfide capture with thiol-containing biotin reagents, enrichment of biotinylated proteins, and identification by liquid chromatography (LC)-MS. ABE has been applied to cultured neurons, synaptosomes, and detergent resistant membranes to identify several hundred putative mammalian palmitoylated proteins[5–6].

The second approach utilizes the commercially available alkyne fatty acid analog 17-octadecynoic acid (17-ODYA), or similarly alkynylated fatty acids, which are metabolically incorporated into endogenous sites of palmitoylation by the cellular palmitoylation machinery[7–8]. 17-ODYA-labeled proteins are then coupled to azide-reporter tags using Huisgen's cycloaddition reaction (click chemistry)[9], allowing for gel-based visualization and MS-identification of palmitoylated proteins. In contrast to ABE, bioorthogonal labeling of palmitoylated proteins with 17-ODYA allows dynamic measurement of the rates of incorporation and turnover by using traditional pulse-chase methods[7, 10]. Furthermore, the natural incorporation of 17-ODYA into proteins in living cells minimizes false positives generated by ABE protocols due to incomplete alkylation of free cysteines or capture of endogenous hydroxylamine-sensitive thioesters.

The proteomic studies using ABE and 17-ODYA methods have, to date, depended on spectral counting. This semi-quantitative technique has, however, impeded a more detailed characterization of dynamic protein palmitoylation events in cells, leaving important questions unanswered. For instance, are all palmitoylation events in cells under dynamic regulation, or, alternatively, might these events be sub-grouped into highly dynamic versus static modifications? Given the inherent lability of the thioester bond, are reversible palmitoylation events regulated by enzymatic and/or non-enzymatic mechanisms in cells? Here we address these questions by combining metabolic incorporation of 17-ODYA and stable isotope labeling of cells (SILAC)[11] for accurate identification and quantitation of specifically enriched palmitoylated proteins. Using this approach, we confidently identified and quantitated more than 400 palmitoylated proteins in mouse T-cell hybridoma cells. We further performed 17-ODYA metabolic pulse-chase labeling to distinguish palmitoylated proteins that undergo rapid turnover from those that are stably modified. Finally, using a lipase-specific inhibitor, we identified a specific set of enzymatically regulated palmitoylated proteins. These findings point to a special population of palmitoylated proteins that, through dynamic regulation by hydrolytic enzymes, are distinguished from bulk protein palmitoylation events.

Results

Quantitative proteomic analysis of protein palmitoylation

To improve the quantitative measurement of palmitoylated proteins, we adapted our 17-ODYA palmitoylated protein enrichment and MS-based proteomics protocol for high-resolution parent ion quantification (MS1) using SILAC (Fig. 1a). In this approach, palmitoylated proteins are identified and quantified by measuring the enrichment ratio across multiple peptides and datasets, greatly expanding the dynamic range to allow accurate quantification of low abundance proteins. We first performed a control experiment where BW5147-derived mouse T-cell hybridoma cells were grown in standard 'light' or isotopically 'heavy' L-arginine (+8) and L-lysine (+10)-containing media, for several

passages, and then each cell preparation was treated overnight with 17-ODYA. The light and heavy-labeled cell pairs were then lysed and their membrane fractions combined at different dilution ratios followed by bioorthogonal coupling to biotin-azide using click chemistry, streptavidin enrichment, trypsin digestion, and multidimensional LC-MS analysis on a high resolution LTQ-Orbitrap Velos instrument. Enriched samples displayed a clearly defined distribution of peptide ratios centered precisely at the dilution factor value (Fig. 1b and c), suggesting even small fractional changes can be accurately quantified.

We next performed two sets of experiments for palmitoylated protein discovery. In the first set (N = 5), heavy cells were treated with 17-ODYA and light cells treated with palmitic acid as a control (Heavy / 17-ODYA, Light / palmitic acid). In the second set (N = 5), the labeling order was reversed (Light / 17-ODYA, Heavy / palmitic acid). Stringent computational thresholds for peak shape, intensity, and co-elution resulted in a reverse-decoy protein false positive rate less than 1%, while providing accurate measurements of proteome-wide enrichment ratios[12] (Methods). Approximately 400 proteins were reciprocally enriched (> 50%) in both experimental groups by 17-ODYA labeling based on the median quantifiable ratio across all peptides assigned and quantified for a specific protein (Supplementary Table 1). In a separate experiment (N = 3), heavy or light 17-ODYA labeled membrane lysates were treated with hydroxylamine, then precipitated and mixed with the equal isotopic paired 17-ODYA labeled membrane lysate (Supplementary Table 2). These experiments identified 338 of the 415 putative palmitoylated proteins, and validate that under these experimental conditions, 17-ODYA is not incorporated into sites of N-myristoylation. In contrast, only 118 palmitoylated proteins were identified in this study with high confidence by spectral counting using previously described thresholds[8] (defined as proteins showing > 5-fold enrichment and > 5 average spectral counts) (Fig. 2a and Supplementary Table 3). Of this group, 117 were found by SILAC, confirming exceptional accuracy (> 99%) for high-confidence spectral counting assignments of palmitoylated proteins. An additional 53 palmitoylated proteins were identified by spectral counting with medium confidence (defined as proteins showing > 5-fold enrichment and 2–5 average spectral counts), of which 47 were also validated by SILAC (> 88% accuracy). By enhancing the quantitation of proteins with only a handful (< 5) of spectra counts, SILAC-based 17-ODYA palmitoylation proteomics identified another 244 palmitoylated proteins that were below the sensitivity limit of spectral counting (Fig. 2b). These results, taken together, demonstrate that SILAC-based quantitation greatly improves the accuracy and sensitivity of 17-ODYA-palmitoylation proteomics, resulting in increased confidence and discovery rate of palmitoylated proteins.

Acyl-fluorophosphonate inhibitors of lipid hydrolases

Protein palmitoylation events are regarded as enzymatically reversible modifications, and candidate protein palmitoyl thioesterases activities have been identified; yet the enzymatic regulation of endogenous palmitoylation events remains poorly characterized. Working with the hypothesis that at least one, and likely several serine hydrolases contribute to enzymatic depalmitoylation of proteins in cells, we sought to develop an inhibitor of this process to globally characterizing the turnover and flux of palmitoylation events in cells.

Approximately 100 serine hydrolases are covalently labeled with the activity-based probe fluorophosphonate-rhodamine (FP-Rh) in mouse proteomes[13]. We hypothesized that candidate protein palmitoyl thioesterases from the serine hydrolase class should prefer an acyl-linked FP that mimics the palmitoyl modification. We synthesized hexadecylfluorophosphonate (HDFP) (Fig. 3a) and its alkynyl derivative hexadecylfluorophosphonate-alkyne (HDFP-alk) (Fig. 3a) as candidate probes for depalmitoylating enzymes. HDFP reactivity with mammalian serine hydrolases was assayed by competitive activity-based protein profiling (ABPP)[14] in mouse brain membrane proteomes using the general activity-based probe FP-Rh (Fig. 3a and b). As predicted, HDFP and HDFP-alk inhibited a specific subset of serine hydrolases. The click chemistry-compatible FP-alkyne (FP-alk)[15] probe reacted with a similar set of serine hydrolases as FP-Rh, but elimination of the internal carbamate narrowed the selectivity of HDFP-alk towards those hydrolases reactive with HDFP. As one specific example, we found that the lysosomal thioesterase PPT1 prefers to react with HDFP-alk over FP-alk (Fig. 3c), indicating that this serine hydrolase preferentially reacts with FP probes that possess a hydrophobic acyl chain resembling its putative acylated substrates. These results, taken together, demonstrate that minor alterations in the FP scaffold can direct reactivity towards distinct subsets of serine hydrolases based on their respective substrate specificities.

We next sought to identify the targets of HDFP using a quantitative LC-MS method termed ABPP-SILAC[16]. Of the fifty serine hydrolases identified by this approach, twenty-one were inhibited (>75%) by incubation with HDFP, including nearly all annotated lipases (Fig. 3d and Supplementary Table 4). In contrast, HDFP did not inhibit most proteases, peptidases, or the proteasome. Overall, these results indicate that HDFP and its clickable analogue HDFP-alk react with a specific subset of serine hydrolases that show a strong preference for lipid substrates and, by extension, designate unannotated serine hydrolases that react with these probes, such as ABHD10, ABHD13, BAT5, and the FAM108 enzymes, as likely lipases.

HDFP effects on dynamic protein palmitoylation

To globally monitor the dynamic turnover of protein palmitoylation events in cells, we first performed a pulse-labeling with 17-ODYA for 2 hours and then chased this pulse with excess palmitic acid for varying time points. 17-ODYA-labeled proteins were initially profiled by click chemistry conjugation to an azide-Rh reporter tag followed by SDS-PAGE and in-gel fluorescence detection. Shorter pulse labeling periods led to less efficient probe incorporation, highlighting a potential limitation of these methods for assaying rapid palmitoylation turnover. Over a timecourse of 6 hours in excess palmitic acid, many, but not all palmitoylated proteins showed a time-dependent decrease in 17-ODYA labeling (Fig. 4a). These pulse-chase conditions may not fully reflect the endogenous rates of palmitoylation turnover due to residual 17-ODYA resident in cellular lipid pools, but they nonetheless highlight specific proteins with accelerated palmitoylation turnover using a simple and rapid non-radioactive assay.

We next treated cells with HDFP or DMSO along with 17-ODYA for various times, followed by click conjugation to an azide-Rh tag and gel-based analysis. A clear time-

dependent enhancement of protein palmitoylation was observed in HDFP-treated T-cells (Fig. 4b) and HEK293T cells (Supplementary Fig. 1a and b). Treatment with a non-reactive control probe 1-heptadecanol (C_{17}-OH) did not change the extent of 17-ODYA labeling of proteins (Fig. 4c). These results suggested that HDFP prevents the steady-state turnover of palmitoylation events in cells, but other interpretations were possible. For instance, HDFP could block enzymes responsible for hydrolyzing palmitoyl-CoA, which could generate more substrate for producing palmitoylated proteins. To more directly determine whether HDFP blocked the turnover of palmitoylated proteins, cells were pulsed with 17-ODYA for 2 hours and then chased with a treatment of palmitic acid and DMSO or palmitic acid and HDFP for 1–6 hr. Interestingly, a discrete subset of palmitoylated proteins were identified that showed rapid loss of signals in DMSO-treated cells, but stable signals in HDFP-treated T-cells (Fig. 4d, marked with a 1) or HEK293T cells (Supplementary Fig. 1c), pointing to a group of proteins bearing dynamic palmitoylation events that were regulated by HDFP-sensitive serine hydrolases. Other classes of palmitoylated proteins were also identified, including those that showed minimal turnover in this pulse-chase experiment (Fig. 4d, marked with a 3) and those with decreasing 17-ODYA signals that were only partially protected by HDFP (Fig. 4d, marked with a 2). HDFP also protected the palmitoylation turnover of transiently overexpressed wild-type HRAS in HEK293T cells (Supplementary Fig. 1d). These results provide further evidence that palmitoylation events exhibit markedly different turnover rates in cells and indicate that a subset of the more dynamic events are regulated by serine hydrolases.

Proteomic profiling of dynamic protein palmitoylation

We next set out to identify proteins that rapidly cycle their palmitoylation state using quantitative (SILAC) proteomic analysis of 17-ODYA pulse-chase-labeled cells. Heavy and light-labeled cells were treated for 2 hours with 17-ODYA, then one isotopic state was harvested and the other was placed in chase media for 4 hours. Due to the abbreviated 17-ODYA treatment period and extended chase time, the overall sensitivity for detecting palmitoylated proteins was reduced compared to our standard proteomic analysis of 17-ODYA-labeled cells, but we still acquired quantitative information on 309 of the 415 palmitoylated proteins identified in our initial studies (Supplementary Tables 5 and 6). Cycloheximide was added during the chase period to prevent ratio changes due to changes in gene transcription or protein translation, although as a consequence, an additional variable for protein stability was introduced. This was addressed by performing unenriched quantitative proteomics on membrane lysates for each sample pair (N = 2) (Supplementary Table 7). This experiment yielded abundance measurements for 213 of the initial 415 palmitoylated proteins, of which only nine were found to be altered in expression level by > 2-fold after the 4 hour chase period (Supplementary Tables 5 – 7). Many well-characterized palmitoylated proteins, including HRAS/NRAS and GNAS were confirmed as targets of dynamic palmitoylation turnover. In total, ~80 palmitoylated proteins showed at least a 2-fold decrease in 17-ODYA enrichment over the course of 4 hours, indicative of rapid cycling of their palmitoylation modifications.

We next tested the contribution of hydrolytic enzymes to palmitoylation turnover by coupling pulse-chase methods with HDFP treatment. After 2 hours of 17-ODYA labeling,

pairs of light and heavy SILAC-labeled cells were placed in chase media with DMSO or HDFP for 4 hours, respectively. Palmitoylated proteins were then enriched and quantified by SILAC, providing quantitative data on 328 of the 415 assigned palmitoylated proteins. Approximately 50 of these 328 palmitoylated proteins were protected from turnover by HDFP (ratio > 1.5) over the course of 4 hours (Supplementary Tables 5 and 8). Importantly, the vast majority of palmitoylated proteins showed only a minor change in palmitoylation turnover after HDFP treatment, indicating that serine hydrolase-mediated turnover of protein palmitoylation is not a general phenomenon, but directed toward a specific subset of dynamically palmitoylated proteins.

In combination, these two proteomics experiments globally defined both 1) highly dynamic protein palmitoylation events, and 2) the subset of these events that are regulated by serine hydrolases. Figure 5a shows the MS1 spectra for a representative serine hydrolase-regulated, dynamically palmitoylated protein ubiquitin-like protein 3 (UBL3), where reciprocal responses were observed in replicate experiments where the order of treatment was reversed in light and heavy cells for Experiment 1 and Experiment 2. In total, about 2/3 (281) of the assigned palmitoylated proteins were successfully quantified in both pulse-chase proteomics experiments, of which about two dozen proteins showed evidence of substantial turnover (> 2-fold) that was serine hydrolase-mediated as defined by HDFP protection (>1.5-fold) during the 4 hour pulse (Fig. 5b, red circles, and Supplementary Fig. 2). A survey of these serine hydrolase-regulated palmitoylated proteins revealed they are enriched in certain protein classes, such as the ras family GTPases, G-proteins (including GNAS and GNA13), membrane-associated guanylate kinase (MAGUK) proteins (MPP1 and MPP6), leucine-rich repeat and PDZ domain (LAP) proteins (ERBB2IP and SCRIB), and the cancer-related transmembrane protein metadherin (MTDH)[17]. A distinct set of proteins showed rapid turnover that was not stabilized by HDFP (Fig. 5b, green circles). Many of these proteins were found to decrease in abundance over the 4 hour timecourse (FXYD5, ERO1, HSP90B1, TUBB4, etc.), suggesting that their changing signals are due to protein (rather than palmitoylation) turnover, although the possibility remains that at least some of them contain dynamic palmitoylation events that are regulated by HDFP-insensitive enzymes. The fast-cycling, HDFP-sensitive palmitoylation events were, as a whole, exceptional in that palmitoylation proved to be a rather stable post-translational modification for the majority of proteins detected in our study (> 75%) (Fig. 5b, black circles). Thus, somewhat surprisingly, enzymatically regulated dynamic palmitoylation is not widespread, but targeted to specific proteins, in particular, those with annotated roles in cell growth, migration, and cancer.

Discussion

Palmitoylation is generally thought to be dynamically regulated[3, 18], although the extent to which this applies to all palmitoylated proteins and the mechanisms that control turnover of this lipid modification remain poorly characterized. The palmitoylated proteins PSD-95[19], GNAS[20], and HRAS[21] each demonstrate accelerated palmitoylation turnover following receptor stimulation, although until now there has been limited evidence that this phenomenon is enzymatically regulated. Two serine hydrolases, LYPLA1[22] and PPT1[23], have been identified from cell lysates as candidate enzymes capable of hydrolyzing palmitoylated HRAS *in vitro*, but whether endogenous HRAS or other palmitoylated

proteins are physiologic substrates for LYPLA1 in living cells remains unknown. Recent pharmacological evidence has also been put forth to support that LYPLA1 is responsible for dynamic palmitoylation turnover of HRAS[24]. On the other hand, siRNA knockdown of LYPLA1 in mammalian cells fails to change the sub-cellular localization of fluorescently tagged palmitoylated proteins with statistical significance[24]. Given these somewhat conflicting observations on studies of individual palmitoylated proteins and candidate protein palmitoyl thioesterases, we sought to examine dynamic turnover of protein palmitoylation events in cells using a more global proteomic approach that exploited polypharmacology inhibitors targeting several lipase members of the serine hydrolase class.

Among the dynamically palmitoylated proteins identified in our study were GNAS and HRAS/NRAS, corroborating previous reports that these proteins show accelerated palmitoylation cycling[20–21]. Interestingly, if we examine unique peptides from either NRAS or HRAS, and ignore common shared peptides, we find that NRAS is exceptionally dynamic in both Experiment 1 (9.80 ± 1.03) and Experiment 2 (5.73 ± 0.63), while HRAS shows much smaller ratio changes in either Experiment 1 (1.70 ± 0.11) or Experiment 2 (1.87 ± 0.27): One explanation for this discrepancy is the recent observation that HRAS, but not NRAS, is a target of FKBP12-mediated proline isomerization, which is essential for rapid HRAS depalmitoylation[25]. Given that our experiments include cycloheximide (an inhibitor of FKBP12) during the chase period, we expect proline isomerization of HRAS will be blocked and thus prevent rapid palmitoylation turnover. Considering the important roles that RAS proteins and other dynamically palmitoylated proteins identified in this study play in cell polarity[26], signaling and diseases like cancer[27–28], the development of specific small-molecule inhibitors of their palmitoylation turnover could have tremendous value for basic and translational research.

We see several exciting avenues for future research on dynamic palmitoylation using our approach described here. For instance, while our current results have identified proteins that show inherently dynamic palmitoylation events, cell stimulation is also known to modulate protein palmitoylation. Global pulse-chase proteomic methods could thus be used to reveal context-dependent changes in protein palmitoylation induced by specific cellular signaling pathways. An additional area of interest is the identification of serine hydrolases responsible for regulating protein palmitoylation events in cells. Finally, further advances in MS-based methods should enable site-specific detection of dynamic palmitoylation events, which would be particularly valuable for proteins that bear multiple palmitate modifications, only a subset of which may be dynamically regulated.

Methods

Cell culture

BW5147-derived mouse T-cell hybridoma cells were grown in RPMI 1640 (Mediatech) supplemented with 10% fetal bovine serum (FBS) (Gemini) and 1% penicillin-streptomycin-glutamate (PSQ) (Invitrogen). Cells were passaged six times in RPMI-1640 minus L-Lysine and L-Arginine (Thermo) supplemented 10% dialyzed FBS (Gemini), 1% PSQ, and 100 μg / mL [$^{13}C_6$,$^{15}N_4$] L- Arginine-HCl and [$^{13}C_6$,$^{15}N_2$] L-Lysine-HCl (Aldrich) or L-Arginine-HCl and L-Lysine-HCl (Sigma) and cell aliquots were frozen and replaced periodically.

HEK293T cells were cultured in DMEM (High Glucose) supplemented with 10% FBS and 1% PSQ and transfected using Fugene HD transfection reagent (Roche).

Metabolic labeling with 17-ODYA

17-ODYA (Cayman) was dissolved in DMSO to make a 20 mM stock solution. To identify 17-ODYA labeled proteins, approximately 2.5×10^7 of both heavy and light cells were labeled overnight with either 20 μM 17-ODYA or 20 μM palmitic acid added directly to the growth media. Cell were collected by centrifugation at 500× g and washed 2× with PBS, and then frozen as a pellet at −80°C. For fluorescent gel-based pulse-chase analysis, mouse T-cell hybridoma cells were labeled in RPMI 1640 supplemented with 10% dialyzed FCS, 1% PSQ, and 20 μM 17-ODYA. Cells were labeled for 2 hours, and then washed in PBS. Chase media was prepared containing RPMI 1640, 10% dialyzed FCS, 1% PSQ, and 250 μM final palmitic acid. Extensive sonication was required to dissipate visible particulates. DMSO or 20 μM HDFP (20 mM stock solution in DMSO) were mixed with the chase media, added to the 17-ODYA labeled cells, and aliquots were collected at the described time points. For SILAC pulse-chase proteomic experiments, heavy and light cells were pulsed for 2 hours in 17-ODYA, either frozen or then chased for 4 hours in chase media with DMSO or 20 μM HDFP.

17-ODYA lysate preparation, click chemistry, and enrichment

Frozen cell pellets were resuspended in PBS with 20 μM HDFP, sonicated, and separated into soluble and insoluble (membrane) fractions by ultracentrifugation at 100,000× g for 45 minutes. The insoluble pellet was sonicated in PBS and the protein concentration was determined using the BCA protein assay on a microplate reader. For fluorescent gel-based analysis, 50 μg of lysate was mixed with 20 μM rhodamine-azide, 1 mM Tris(2-carboxyethyl)phosphine (TCEP, Sigma-Aldrich), 100 μM Tris[(1-benzyl-1H-1,2,3-triazol-4-yl)methyl]amine (TBTA) (Sigma-Aldrich), and 1 mM CuSO4 in PBS in a 50 μL at room temperature. After 1 hour, samples were mixed with SDS sample loading buffer and loaded without boiling on a 10% SDS-PAGE gel, separated over 850 volt-hours, and analyzed using a Hitachi FMBIO-II flatbed fluorescence scanner. For proteomic analysis, 1 – 1.5 mg of both light and heavy membrane proteomes were mixed equally in a 1:1 ratio, then extracted once with chloroform:methanol to remove lipids and unincorporated probe. To test if labeling is hydroxylamine sensitive, heavy (or light) pairs of 17-ODYA labeled membrane lysates were treated with or without 1 M hydroxylamine for 5 minutes on a 90°C heat block. Following this treatment, control and hydroxylamine samples were precipitated with chloroform:methanol and washed 2 x with cold methanol, and then mixed and sonicated in PBS. For each set of experiments, the precipitated proteome was sonicated in PBS and combined with 500 μM biotin-azide, 100 μM TBTA, 1 mM TCEP, and 1 mM CuSO4 in 2 mL PBS for 1 hour. Samples were centrifuged for 4 minutes at 8000 rpm to pellet the precipitated protein, washed 1× with cold methanol, and extracted 1× with chloroform/methanol. The protein interphase was then washed with cold methanol and solubilized in 6 M urea in PBS. Next, 10 mM neutral TCEP was added for 30 minutes followed addition of 20 mM iodoacetamide for 30 minutes. SDS was added to a final concentration of 2%, and the sample was diluted 10× in PBS. Streptavidin beads (Thermo) (100 μL slurry) were added and rotated at room temperature for 2 hours. Beads were transferred to Bio-spin filters

(BioRad) and coupled to a vacuum manifold and washed with 10× 1mL 1% SDS in PBS, then 20× 1mL PBS. Beads were transferred to screw-top eppendorf tubes and resuspended in 2 M urea/PBS supplemented with 1 mM calcium chloride and sequence grade porcine trypsin (Promega) for overnight digestion at 37 °C. The eluant was collected the following day and acidified with 5% formic acid.

Serine hydrolase activity-based profiling

Fluorescent gel-based analysis of serine hydrolase activities was performed as previously described[13]. Briefly, 50 μg of mouse brain membrane proteome was incubated with 2 μM FP-alk, HDFP, or HDFP-alk for 30 minutes in 50 μL of PBS, then FP-TAMRA (2 μM) was added for 1 hour. Samples were boiled in SDS loading buffer and separated by SDS-PAGE for 850 volt-hours and analyzed on a flatbed fluorescence scanner. Similar competitive analysis was performed using FP-alk and HDFP-alk followed by click chemistry (as described above) with rhodamine-azide. The selectivity of HDFP was profiled using SILAC quantitative competitive activity-based profiling. Heavy and light T-cell hybridoma cells were treated with DMSO or 20 μM HDFP for 4 hours in culture, then washed, sonicated, and fractionated into soluble and insoluble fractions by ultracentrifugation. Heavy and light proteomes were mixed in a 1:1 ratio according to the calculated protein concentration and mixed with 5 μM FP-Biotin for 1 hour. Excess unreacted FP-Biotin was removed over a PD-10 column (GE Healthcare), and the proteome was denatured in 1% SDS-PBS, boiled, and mixed with streptavidin beads for enrichment as described above. To measure protein turnover in unenriched samples, 50 μg of each heavy and light membrane proteome pair were mixed and extracted 2× with chloroform:methanol, then resuspended in 2M urea 25 mM bicarbonate buffer for overnight trypsin digestion.

Mass spectrometry

Mass spectrometry was performed using a Thermo Orbitrap Velos mass spectrometer. Peptides were eluted using a 6-step MudPIT protocol (using 0%, 10%, 25%, 50%, 80%, and 100% salt bumps of 500 mM aqueous ammonium acetate, each step followed by an increasing gradient of aqueous acetonitrile/0.1% formic acid) and data were collected in data-dependent acquisition mode (2 MS1 microscans (400–1800 m/z) and 30 data-dependent MS2 scans) with dynamic exclusion enabled (repeat count of 1, exclusion duration of 20 s) with monoisotopic precursor selection enabled. All other parameters were left at default values. Unenriched samples were eluted in a 12-step MudPIT using (0%, 5%, 10%, 20%, 30%, 40%, 50%, 60%, 70%, 80%, 90% and 100%) salt bumps of 500mM ammonium acetate. SEQUEST searches allowed for variable oxidation of methionine (+15.9949), static modification of cysteine residues (+57.0215 due to alkylation), and no enzyme specificity. Each data set was independently searched with light and heavy params files; for the light search, all other amino acids were left at default masses; for the heavy search, static modifications on lysine (8.0142) and arginine (10.0082) were specified. The precursor ion mass tolerance was set to 50 ppm and the fragment ion mass tolerance was left at the default assignment of 0. The data was searched using a mouse reverse-concatenated non-redundant (gene-centric) FASTA database that combines IPI and Ensembl identifiers, containing 23,420 unique entries. The resulting MS2 spectra matches were assembled into protein identifications and filtered using DTASelect (version 2.0.47) with the --trypstat

option, which applies different statistical models for the analysis of tryptic, half-tryptic, non-tryptic peptides. Peptides were also restricted to fully tryptic using the -y 2 option with a defined peptide false positive rate of 2% (--fp 0.02) and single peptides per locus were allowed (-p 1). Redundant peptide identifications common between multiple proteins were allowed, but the database was restricted to a single consensus splice variant. SILAC ratios were quantified using in-house software as described[12]. In short, extracted MS1 ion chromatograms (+/− 10 ppm) from both "light" and "heavy" target peptide masses (m/z) are generated using a retention time window (+/− 10 minutes) centered on the time when the peptide ion was selected for MS/MS fragmentation, and subsequently identified. Next, the ratio of the peak areas under the light and heavy signals (signal-to-noise ratio S/N >2.5) are calculated. Multiple computational filters are used to ensure that the correct peak-pair is used for quantification, including a co-elution correlation score filter ($R^2 \geq 0.8$) that removes target peptides with bad co-elution profile, and an "envelope correlation score" filter ($R^2 > 0.8$) that eliminates target peptides whose predicted pattern of the isotopic envelope distribution does not match the experimentally observed high-resolution MS1 spectrum. Additionally, the software was updated to identify cases where complete inhibition could not be quantified based on light/heavy peak pairs due the absence of a MS1 signal from either the heavy or light sample. In order to identify these cases, all single MS1 chromatographic peaks (from either the light or the heavy sample) were identified within a retention time window. Next, these peaks were aligned with the corresponding sequence SEQUEST/DTASelect identification and the charge state and monoisotopic mass were validated using the "envelope correlation score" filter[12]. Finally, the candidate peak was cross-checked to ensure there was no corresponding (heavy or light) peak co-eluting around the same retention time window. Only after all these conditions are met, the peptide was assigned as the case of complete inhibition with an artificial threshold ratio of 20. To identify 17-ODYA enriched proteins, two experiments were performed. Light and heavy cells were treated with 17-ODYA and palmitic acid respectively (N=5). The inverse experiment was next performed, where light cells were treated with palmitic acid and heavy cells with 17-ODYA (N=5). If the median peptide ratio pooled from both experiments was greater or equal to 1.5, and there were quantified peptides from both reciprocal experiments, the protein is considered to be palmitoylated. In subsequent experiments, singleton values were not included in mean calculations or in the number of quantitated peptides used for calculating standard errors.

Synthetic methods

Synthetic methods are described in the Supplementary Note.

Supplementary Material

Refer to Web version on PubMed Central for supplementary material.

Acknowledgments

We would like to thank Sandra Hofmann (UT Southwestern) for providing purified PPT1 enzyme, Anna Spears and Melissa Dix for mass spectrometry assistance, and members of the Cravatt lab for helpful discussions. Funding was provided by the National Institutes of Health (CA087660), F32NS060559 (B.R.M.), K99CA151460 (B.R.M.),

DRG1978-08 (S.E.T.), Deutscher Akademischer Austausch Dienst (A.A.), and The Skaggs Institute for Chemical Biology.

References

1. Schmidt MFG, Schlesinger MJ. Fatty acid binding to vesicular stomatitis virus glycoprotein: a new type of post-translational modification of the viral glycoprotein. Cell. 1979; 17:813–819. [PubMed: 226266]
2. Schlesinger M, Magee A, Schmidt M. Fatty acid acylation of proteins in cultured cells. J Biol Chem. 1980; 255:10021–10024. [PubMed: 7430112]
3. Smotrys JE, Linder ME. PALMITOYLATION OF INTRACELLULAR SIGNALING PROTEINS: Regulation and Function. Annual Review of Biochemistry. 2004; 73:559–587.
4. Wan J, Roth AF, Bailey AO, Davis NG. Palmitoylated proteins: purification and identification. Nat Protoc. 2007; 2:1573–1584. [PubMed: 17585299]
5. Yang W, Di Vizio D, Kirchner M, Steen H, Freeman MR. Proteome Scale Characterization of Human S-Acylated Proteins in Lipid Raft-enriched and Non-raft Membranes. Molecular & Cellular Proteomics. 2010; 9:54–70. [PubMed: 19801377]
6. Kang R, et al. Neural palmitoyl-proteomics reveals dynamic synaptic palmitoylation. Nature. 2008; 456:904–909. [PubMed: 19092927]
7. Hang HC, et al. Chemical probes for the rapid detection of Fatty-acylated proteins in Mammalian cells. J Am Chem Soc. 2007; 129:2744–2745. [PubMed: 17305342]
8. Martin BR, Cravatt BF. Large-scale profiling of protein palmitoylation in mammalian cells. Nat Methods. 2009; 6:135–138. [PubMed: 19137006]
9. Speers AE, Cravatt BF. Profiling enzyme activities in vivo using click chemistry methods. Chem Biol. 2004; 11:535–546. [PubMed: 15123248]
10. Zhang MM, Tsou LK, Charron G, Raghavan AS, Hang HC. Tandem fluorescence imaging of dynamic S-acylation and protein turnover. Proceedings of the National Academy of Sciences. 2010; 107:8627–8632.
11. Ong SE, et al. Stable Isotope Labeling by Amino Acids in Cell Culture, SILAC, as a Simple and Accurate Approach to Expression Proteomics. Mol Cell Proteomics. 2002; 1:376–386. [PubMed: 12118079]
12. Weerapana E, et al. Quantitative reactivity profiling predicts functional cysteines in proteomes. Nature. 2010; 468:790–795. [PubMed: 21085121]
13. Bachovchin DA, et al. Superfamily-wide portrait of serine hydrolase inhibition achieved by library-versus-library screening. Proceedings of the National Academy of Sciences. 2010; 107:20941–20946.
14. Leung D, Hardouin C, Boger DL, Cravatt BF. Discovering potent and selective reversible inhibitors of enzymes in complex proteomes. Nat Biotechnol. 2003; 21:687–691. [PubMed: 12740587]
15. Tully SE, Cravatt BF. Activity-based probes that target functional subclasses of phospholipases in proteomes. J Am Chem Soc. 2010; 132:3264–3265. [PubMed: 20178358]
16. Adibekian A, et al. Click-generated triazole ureas as ultrapotent in vivo active serine hydrolase inhibitors. Nat Chem Biol. 2011; 7:469–478. [PubMed: 21572424]
17. Yoo BK, et al. Astrocyte elevated gene-1 (AEG-1): A multifunctional regulator of normal and abnormal physiology. Pharmacol Ther. 2011
18. Fukata Y, Fukata M. Protein palmitoylation in neuronal development and synaptic plasticity. Nat Rev Neurosci. 2010; 11:161–175. [PubMed: 20168314]
19. El-Husseini Ael D, et al. Synaptic strength regulated by palmitate cycling on PSD-95. Cell. 2002; 108:849–863. [PubMed: 11955437]
20. Wedegaertner PB, Bourne HR. Activation and depalmitoylation of Gs[alpha]. Cell. 1994; 77:1063–1070. [PubMed: 7912657]
21. Baker TL, Zheng H, Walker J, Coloff JL, Buss JE. Distinct Rates of Palmitate Turnover on Membrane-bound Cellular and Oncogenic H-Ras. J Biol Chem. 2003; 278:19292–19300. [PubMed: 12642594]

22. Duncan JA, Gilman AG. A Cytoplasmic Acyl-Protein Thioesterase That Removes Palmitate from G Protein alpha Subunits and p21RAS. J Biol Chem. 1998; 273:15830–15837. [PubMed: 9624183]
23. Camp L, Hofmann S. Purification and properties of a palmitoyl-protein thioesterase that cleaves palmitate from H-Ras. J Biol Chem. 1993; 268:22566–22574. [PubMed: 7901201]
24. Dekker FJ, et al. Small-molecule inhibition of APT1 affects Ras localization and signaling. Nat Chem Biol. 2010; 6:449–456. [PubMed: 20418879]
25. Ahearn IM, et al. FKBP12 Binds to Acylated H-Ras and Promotes Depalmitoylation. Molecular Cell. 2011; 41:173–185. [PubMed: 21255728]
26. Quinn BJ, et al. Erythrocyte scaffolding protein p55/MPP1 functions as an essential regulator of neutrophil polarity. Proceedings of the National Academy of Sciences. 2009; 106:19842–19847.
27. Wennerberg K, Rossman KL, Der CJ. The Ras superfamily at a glance. Journal of Cell Science. 2005; 118:843–846. [PubMed: 15731001]
28. Konstantinopoulos PA, Karamouzis MV, Papavassiliou AG. Post-translational modifications and regulation of the RAS superfamily of GTPases as anticancer targets. Nat Rev Drug Discov. 2007; 6:541–555. [PubMed: 17585331]

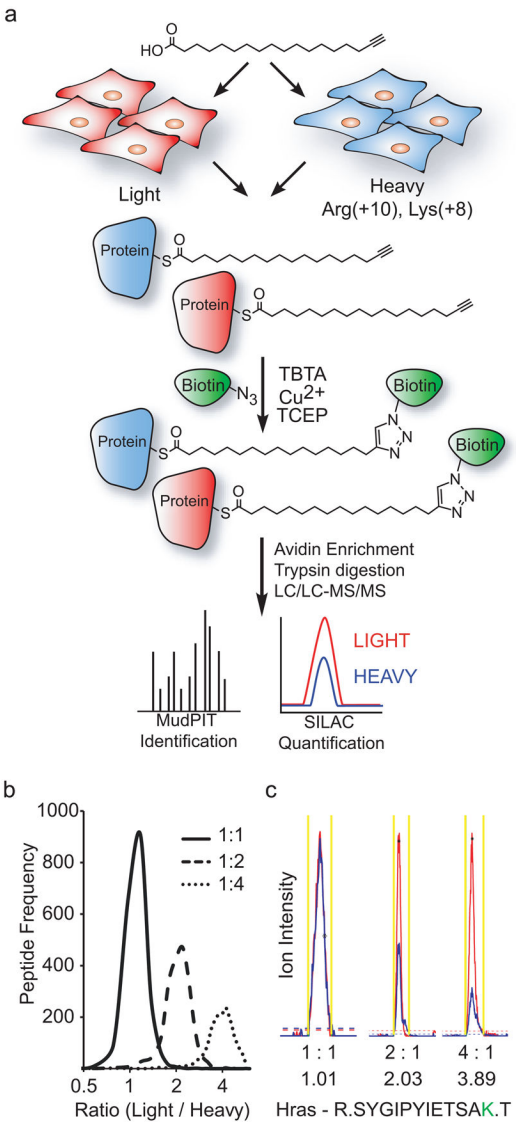

Figure 1. Quantitative analysis of protein palmitoylation

(**a**) SILAC-labeled heavy (blue) and light (red) cells are metabolically labeled with 17-ODYA, lysed and mixed at a 1:1 ratio for click chemistry ligation to biotin-azide for enrichment and quantitative proteomic analysis. (**b**) Global distribution of enriched peptide ratios after mixing membrane lysates at pre-defined ratios. Data is displayed using a log(2) scale on the x-axis. Only peptides identified as specifically enriched by the criteria described in the **Methods** are displayed. (**c**) Parent ion spectra (MS1) for a specific peptide from the palmitoylated protein HRAS at different dilution ratios. Light (red) and heavy (blue) spectra are shown at each dilution. Yellow and dashed lines represent the computationally defined peak and baseline respectively used for integration and quantification. The defined dilutions and the calculated experimental ratios are displayed below the individual peak spectra, respectively. The lysine in the peptide sequence is colored green to represent the isotopic amino acid.

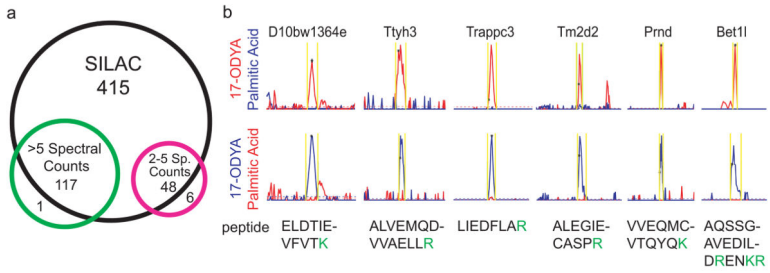

Figure 2. Enhanced assignment of palmitoylated proteins using SILAC 17-ODYA proteomics

(**a**) Overlap of high-confidence palmitoylated protein assignments by SILAC and spectral counting from 17-ODYA labeled T-cell membrane lysates. (**b**) Representative mass spectra for six proteins identified only by SILAC quantification. D10BW1364E (FAM108B), TTYH3 (tweety homologue 3), TRAPPC3 (trafficking protein particle complex 3), T2MD2 (beta-amyloid-binding protein-like 1), PRND (prion protein 2), and BET1L (blocked early in transport 1 homologue-like) all show selective enrichment in SILAC samples with 17-ODYA-labeled light or heavy cells. Yellow lines represent computationally defined peak used for quantification. Blue spectra represent heavy peptides and red spectra represent from light peptides. Green letters in the peptide sequences represent isotopically labeled amino acids.

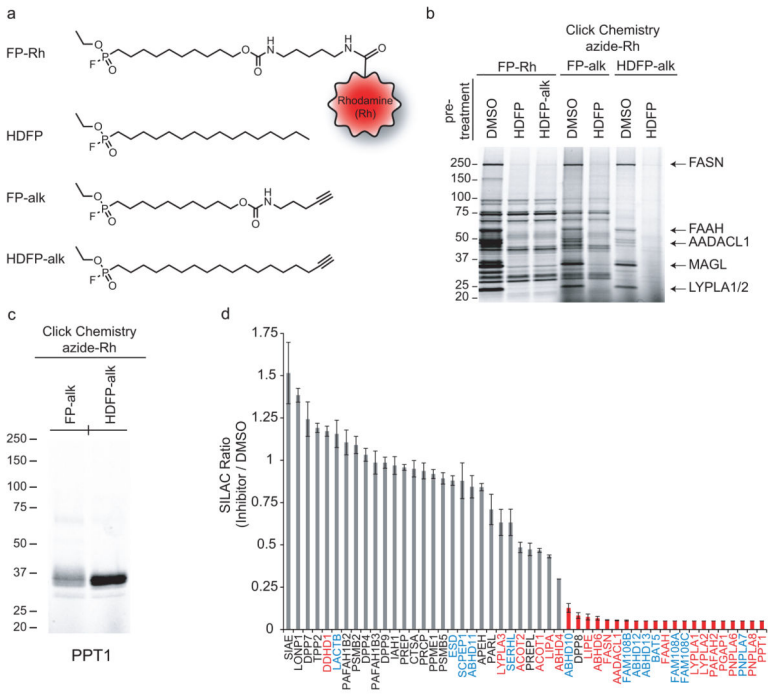

Figure 3. HDFP is a lipase-selective inhibitor

(**a**) Structures of fluorophosphonate (FP) activity-based probes and the lipase-directed inhibitors HDFP and HDFP-alk. Tetramethyl-6-Carboxyrhodamine (TAMRA) is shown as a cartoon in red. (**b**) Competitive ABPP to survey serine hydrolase targets of HDFP. A mouse brain membrane proteome was pre-incubated with the described inhibitors for 30 minutes, and then labeled with the indicated activity-based probes for competitive gel-based ABPP. Arrows highlight annotated lipases that were inhibited by HDFP and labeled by HDFP-alk (detected by click chemistry conjugation to an azide-Rh tag). (**c**) PPT1 is selectively inhibited by HDFP-alk. Purified human PPT1 (5 ng) was incubated with 5μM FP-alk of HDFP-alk, and then reacted with azide-Rh for fluorescent gel-based analysis. (**d**) Competitive ABPP SILAC to identify serine hydrolase targets of HDFP. Mouse T-cell hybridoma lysates were fractionated into membrane and soluble proteomes for separate analysis. Peptides with MS1 peaks passing stringent size and shape thresholds, but that lacked a signal in the HDFP-treated light or heavy sample were assigned a lower-limit ratio of 0.05 (HDFP / DMSO). Protein with bars colored red represent enzymes inhibited by >75%. Protein IDs in red type highlight annotated lipases and protein IDs in blue type highlight unannotated serine hydrolases. Error bars, s.e.m. (N = 4).

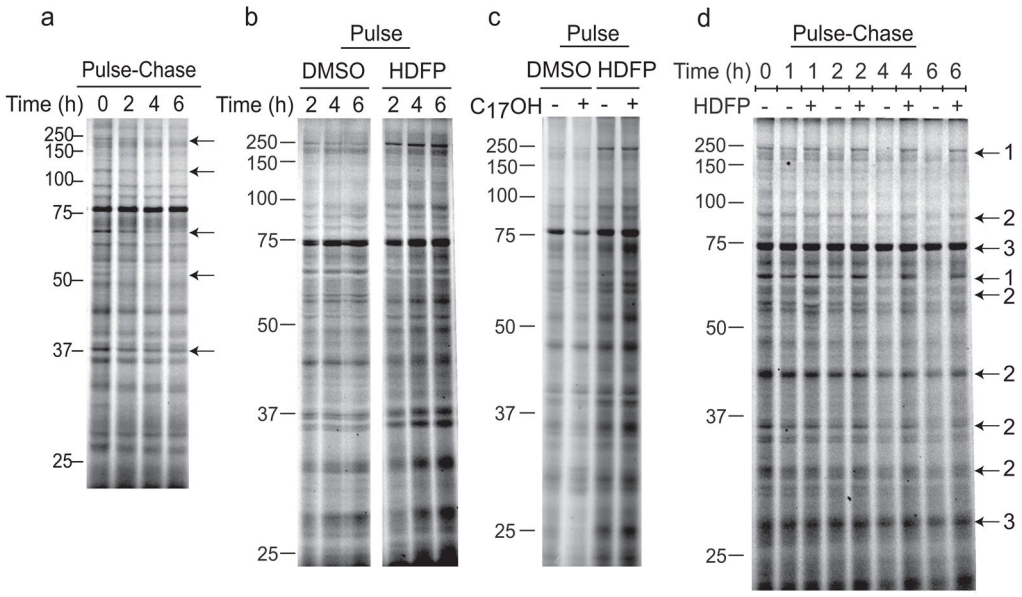

Figure 4. Lipase inhibition by HDFP enhances 17-ODYA labeling and prevents palmitoylation turnover

(**a**) Pulse-chase labeling of T-cell hybridoma cells identifies specific proteins that possess dynamic palmitoylation events that are rapidly turned over. Cells were pulsed in 17-ODYA for 2 hours, then washed and placed in 'chase' media containing excess palmitic acid for the times periods described. Arrows highlight protein with rapid palmitoylation turnover observed by pulse-chase labeling. (**b**) HDFP enhances 17-ODYA labeling. Cells treated with HDFP show a time-dependent increase in the extent of 17-ODYA labeling in T-cell hybridoma cells. (**c**) 1-heptadecanol (C_{17}-OH) does not change the labeling efficiency after 6 hours of treatment with 17-ODYA in the presence or absence of HDFP. (**d**) HDFP prevents palmitoylation turnover on specific proteins. Cells were pulsed with 17-ODYA for 2 hours, then washed and chased with or without HDFP, demonstrate a time-dependent stabilization of 17-ODYA labeling on a subset of labeled proteins. Arrows highlight three representative classes of palmitoylated proteins: (1) complete protection by HDFP, (2) partial protection by HDFP, and (3) no protection by HDFP.

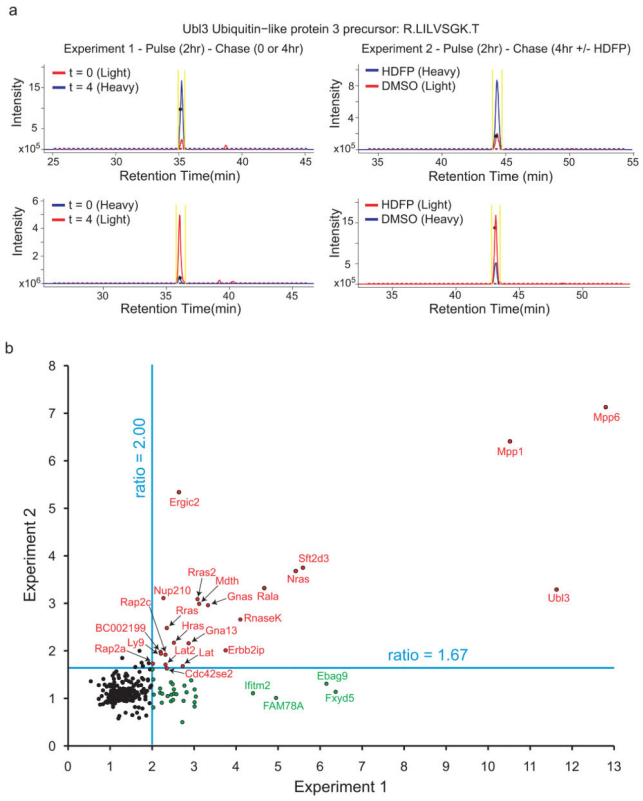

Figure 5. Enzymatically regulated, dynamically cycling palmitoylated proteins

(**a**) Representative MS1 spectra from the UBL3 tryptic peptide extracted from reciprocal experiments reversing the treatment order between heavy and light cells. Yellow and dashed lines represent the computationally defined peak and baseline for integration. Red spectra represent light peptides and blue spectra represent heavy peptides. (**b**) SILAC ratios for two experiments are plotted. In experiment 1, cells were labeled with 17-ODYA (2 hrs) and harvested or placed in 'chase' media for an additional 4 hours. The ratio is displayed as t = 0 h / t = 4 h, combining 3 replicates where each isotopic pair was treated inversely, and totaling 6 biological replicates. In Experiment 2, cells were labeled for 2 hrs with 17-ODYA, then placed in chase media for 4 hrs with DMSO or HDFP. The ratio is displayed as HDFP / DMSO, and is pooled from combining 4 replicated where each isotopic pair was treated inversely, totaling 8 biological replicates. For both experiments, proteins were filtered to include only assigned palmitoylated proteins (Supplementary Table 1). Reference lines were added to delineate thresholds for assigning dynamically palmitoylated proteins. FAM49B and SCRIB were maximally changed in each experiment (assigned an upper limit ratio of 20), and hence off-scale. Protein labeled in red are considered dynamically palmitoylated and regulated by targets of HDFP (high ratios in Experiments 1 and 2). Proteins labeled in green demonstrate rapid palmitoylation turnover in Experiment 1, but show no stabilization upon HDFP treatment in Experiment 2.